Crystallographically driven Au catalyst movement during growth of InAs/GaAs axial nanowire heterostructures

Mohanchand Paladugu,[1] Jin Zou,[1,2,a)] Ya-Nan Guo,[1] Xin Zhang,[1] Hannah J. Joyce,[3] Qiang Gao,[3] H. Hoe Tan,[3] C. Jagadish,[3,a)] and Yong Kim[4]
[1]*School of Engineering, The University of Queensland, St Lucia, Queensland 4072, Australia*
[2]*Centre for Microscopy and Microanalysis, The University of Queensland, St Lucia, Queensland 4072, Australia*
[3]*Department of Electronic Materials Engineering, Research School of Physical Sciences and Engineering, The Australian National University, Canberra, Australian Capital Territory 0200, Australia*
[4]*Department of Physics, Dong-A University, Hadan-2-dong, Sahagu, Busan 604-714, Republic of Korea*

(Received 18 November 2008; accepted 16 February 2009; published online 1 April 2009)

The movement of Au catalysts during growth of InAs on GaAs nanowires has been carefully investigated by transmission electron microscopy. It has been found that Au catalysts preferentially stay on $\{112\}_B$ GaAs sidewalls. Since a {112} surface is composed of a {111} facet and a {002} facet and since {111} facets are polar facets for the zinc-blende structure, this crystallographic preference is attributed to the different interface energies caused by the different polar facets. We anticipate that these observations will be useful for the design of nanowire heterostructure based devices. © *2009 American Institute of Physics*. [DOI: 10.1063/1.3103265]

I. INTRODUCTION

Semiconductor nanowires are ideal nanostructures for exploring new technological applications due to their unique one-dimensional physical properties and, in turn, they are suitable for wide variety of applications.[1,2] The fabrication of axial and radial nanowire heterostructures has further broadened the applications of these nanostructures.[1,2] Many practical applications have been demonstrated using these heterostructures including nanowire diodes,[3] photodiodes,[4] single-electron transistors,[5] and field-effect transistors.[6,7] Nanowires and their associated axial nanowire heterostructures are generally grown via the vapor-liquid-solid mechanism,[8] using metal nanoparticles as the catalysts for the nanowire growth.[9]

Conventional planar heteroepitaxy of different semiconductor materials can produce two-dimensional quantum well heterostructures, and similarly, one-dimensional heterostructures were expected via fabrication of axial nanowire heterostructures.[1] However, since the nanowire growth is mediated by the nanosized metallic catalysts, many extraordinary physical phenomena were observed during the growth of axial nanowire heterostructures compared to their two-dimensional counterparts, such as failure of axial nanowire heterostructure growth and graded heterointerfaces.[10–12] Our recent observations of Au mediated axial growth of InAs on GaAs nanowires revealed that, during the InAs growth, Au catalysts slide down along the {112} sidewalls of GaAs nanowires due to their tendency to preserve an interface with GaAs.[10] This tendency is attributed to the lower Au/GaAs interfacial energy compared to the Au/InAs interfacial energy.[10] Ultimately, this Au particle movement can be stopped when the particle contacts radial overgrowth of InAs. Subsequently Au catalyst-mediated InAs axial growth can be achieved in the form of InAs branches.[11] It is of interest to note that, in almost all the cases, InAs branch growth took place in $\langle 111\rangle_B$ directions at an inclination to the GaAs/InAs core/shell stems that grew in the $[\bar{1}\bar{1}\bar{1}]$ direction,[11] as shown in Fig. 1. It is essential to understand the fundamental mechanism behind this scenario, which can guide us to design and manufacture branched nanostructures with preferred crystallographic directions and desired properties.

In this study, through extensive transmission electron microscopy (TEM) investigations, we determine crystallographic behavior of Au catalysts' movements during growth of InAs on top of GaAs nanowires, where we identified that Au catalysts preferentially retain GaAs $\{112\}_B$ interfaces. The fundamental reason of this physical phenomenon is discussed.

II. EXPERIMENTAL

GaAs epitaxial nanowires were first grown on a $(\bar{1}\bar{1}\bar{1})_B$ GaAs substrate using Au nanoparticles (with a nominal size

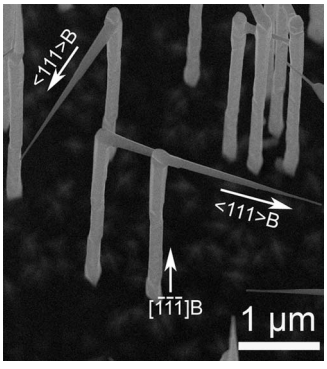

FIG. 1. SEM image of branched InAs/GaAs nanowire heterostructures. The GaAs $(111)B$ substrate normal is tilted 20° away to the electron beam direction.

a)Authors to whom correspondence should be addressed. Electronic addresses: j.zou@uq.edu.au and chennupati.jagadish@anu.edu.au.

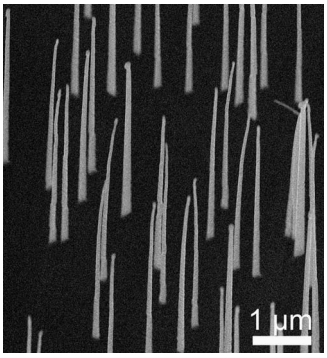

FIG. 2. SEM image of InAs/GaAs nanowire heterostructures with 1 min InAs growth time. The GaAs (111)*B* substrate normal is tilted 20° away to the electron beam direction.

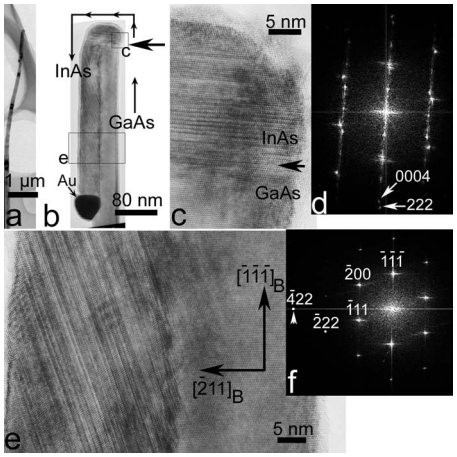

FIG. 3. (a) A low-magnification TEM image of an InAs/GaAs nanowire with its corresponding tip region in (b). (c) HRTEM image showing InAs/GaAs interface region with its corresponding FFT image in (d). (e) HRTEM image showing the downward grown InAs section and its adjacent GaAs section. (f) FFT images taken on the GaAs portion shown in (e).

of ~30 nm) for 30 min in a horizontal flow metal-organic chemical vapor deposition (MOCVD) reactor at 100 mbars with a growth temperature of 450 °C. InAs was then intentionally grown on GaAs nanowires for 1 min at the same growth temperature in order to study the initial behavior of the Au catalysts. Epitaxial GaAs nanowires were grown by flowing trimethylgallium (TMG) and AsH_3 at flow rates of 1.2×10^{-5} and 5.4×10^{-4} mol/min, respectively. InAs nanowire sections were grown by switching off the TMG flow and switching on the trimethylindium flow with a rate of 1.2×10^{-5} mol/min while maintaining the AsH_3 flow as a constant. The fabricated nanowire heterostructures were characterized by high-resolution scanning electron microscopy (SEM) (JEOL 890 with a cold emission gun) and TEM (Philips Tecnai F20). TEM specimens were prepared by ultrasonicating the nanowires in ethanol for 10 min followed by dispersing them onto holey carbon films.

III. RESULTS AND DISCUSSION

Figure 2 shows a typical SEM image of InAs/GaAs nanowire heterostructures, in which the nanowires have grown vertically on the substrate, i.e., along the $[\bar{1}\bar{1}\bar{1}]$ direction. To determine the growth behavior of InAs on GaAs nanowires, particularly the behavior of the Au catalysts, TEM characterizations were carried out. Figure 3(a) shows a low-magnification TEM image of a typical InAs/GaAs nanowire. A downward-sliding Au catalyst can be seen in Fig. 3(a), which induces a nonstraight morphology. Figure 3(b) is a high-magnification TEM image of the nanowire top region and further shows the sliding of the Au catalyst from the nanowire tip. Our extensive TEM investigations showed that over 95% observed nanowires were associated Au sliding. As demonstrated in our earlier studies,[10,13] Au catalysts prefer to retain interfaces with GaAs and this drives the downward growth of InAs nanowires led by the Au catalysts. This growth behavior of InAs is indicated by an arrow in Fig. 3(b). Figure 3(c) is a high-resolution (HR) TEM image of the InAs/GaAs interface region, as indicated in Fig. 3(b). As can be seen, a wurtzite structured segment is sandwiched between two zinc-blende structure segments. To verify the location of InAs/GaAs interface, fast Fourier transform (FFT) (equivalent to the electron diffraction) analysis is performed. Figure 3(d) shows a FFT pattern taken from the interface between the wurtzite structure and the underlying zinc-blende structure. The FFT pattern consists of two sets of diffraction patterns. By careful analysis of the two diffraction patterns, one can determine that the outer set belongs to the zinc-blende structure with the $\langle 110\rangle$ zone axis and the inner set belongs to the wurtzite structure with the $\langle 1\bar{2}10\rangle$ zone axis. An ~7% difference between (222) atomic spacings and (0004) atomic spacings can be determined from the FFT pattern. This analysis indicates that the wurtzite structure shown in Fig. 3(c) belongs to InAs and the underlying zinc-blende structure is GaAs. In addition, the interface between them is atomically sharp.[12]

It has been well documented that InAs and GaAs nanowires grown using MOCVD show different crystal structures. Generally, InAs nanowires show the wurtzite structure, whereas the GaAs nanowires show the zinc-blende structure.[11,12,14] As can be noted from Fig. 3(c), the InAs nanowire section has grown as a zinc-blende structured segment above the wurtzite structured segment. In fact, this phenomenon has been repeatedly observed by our TEM investigations. To understand this, we note that the InAs nanowires grown in the directions other than $\langle 111\rangle_B$ retain the zinc-blende structure.[15,16] As a consequence, we anticipate that the zinc-blende structured InAs segments at the top are caused by the growth direction change during the sideward movement of the Au catalysts.

Figure 3(e) shows a $\langle 110\rangle$ HRTEM image of GaAs with its adjacent InAs, taken from a location marked in Fig. 3(b). The {112} interface between GaAs and InAs can be identified by the presence of strain contrast, and the InAs section consists of many planar defects. According to crystallography, the polarity of the zinc-blende structure leads to the two different {112} surfaces, i.e., $\{112\}_A$ and $\{112\}_B$.[14] To determine the nature of {112} surfaces on which the Au catalyst retains an interface, a FFT pattern was taken from the GaAs nanowire section, as shown in Fig. 3(f), which shows a $\langle 110\rangle$ diffraction pattern. Since the growth direction of GaAs nanowires is along the $[\bar{1}\bar{1}\bar{1}]$ direction, the $(\bar{1}\bar{1}\bar{1})^*$ diffraction spot

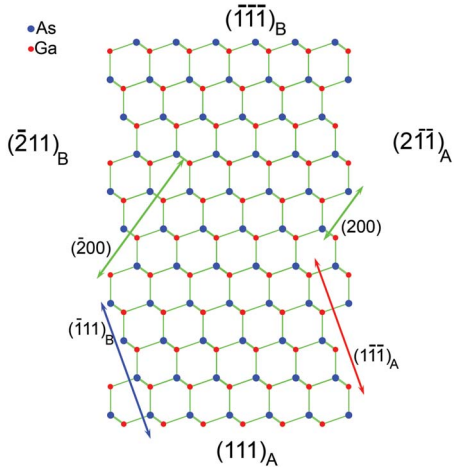

FIG. 4. (Color online) (a) Schematic of the $[01\bar{1}]$ projected GaAs lattice showing $\{111\}_B$ and $\{111\}_A$ planes.

can be uniquely determined, as marked in Fig. 3(f). The nearby $\{200\}^*$ type diffraction spot can be arbitrarily indexed as $(\bar{2}00)^*$ for convenience as such an arbitrary choice would not cause any change in the nature of the $\{112\}$ surfaces. As a consequence, other diffraction spots can be indexed, including $(\bar{4}22)^*$ and $(4\bar{2}\bar{2})^*$. Since for the cubic system the direction of the $[u,v,w]$ zone axis is always parallel to the normal of the (u,v,w) surface (where u,v,w are integers), $[\bar{4}22]$ and $[4\bar{2}\bar{2}]$ directions are, respectively, parallel to the normal of $(\bar{4}22)$ and $(4\bar{2}\bar{2})$ surfaces. Crystallographically speaking, $[\bar{4}22]$ and $[4\bar{2}\bar{2}]$ are along the $\langle 112\rangle_B$ and $\langle 112\rangle_A$, respectively. By comparing Figs. 3(e) and 3(f), we can determine that the Au catalyst retained a $\{112\}_B$ interface with GaAs sidewalls. In fact, our extensive TEM investigations showed that almost all the Au catalysts retained $\{112\}_B$ interfaces with GaAs sidewalls.

To understand why Au catalysts preferentially retain $\{112\}_B$ interfaces with GaAs sidewalls, we analyze the atomic structure of $\{112\}$ surfaces. Figure 4 shows the $[01\bar{1}]$ projected atomic structure of a zinc-blende structure (note that the growth direction of nanowires is $[\bar{1}\bar{1}\bar{1}]$). Two $\{112\}$ surfaces, marked as $(\bar{2}11)$ and $(2\bar{1}\bar{1})$, are shown in Fig. 4. As mentioned earlier, $(\bar{2}11)$ and $(2\bar{1}\bar{1})$ surfaces belong to $\{112\}_B$ and $\{112\}_A$, respectively. It is of interest to note from Fig. 4 that (1) the $\{112\}$ surfaces are not atomically flat and (2) each $\{112\}$ surface can be considered as the composition of zigzag of $\{111\}$ and $\{200\}$ planes. For the $(\bar{2}11)$ surface, the two composing atomic planes are $(\bar{1}11)$ and $(\bar{2}00)$, while for the $(2\bar{1}\bar{1})$ surface, the two composing atomic planes are $(1\bar{1}\bar{1})$ and (200). The $\{200\}$ surfaces are nonpolar surfaces and $(\bar{1}11)$ and $(1\bar{1}\bar{1})$ surfaces, respectively, belong to $\{111\}_B$ and $\{111\}_A$ surfaces. Based on the observed preference for a Au/GaAs$\{112\}_B$ interface, and the interfacial energy argument given in Refs. 10 and 13, we anticipate that the Au/GaAs $\{112\}_B$ interface energy ($\gamma_{\mathrm{Au/GaAs}\{112\}B}$) is lower than the Au/GaAs $\{112\}_A$ interface energy ($\gamma_{\mathrm{Au/GaAs}\{112\}A}$). The fundamental reason of Au preferentially retaining interfaces with $\{112\}_B$ sidewalls of GaAs nanowires should be due to

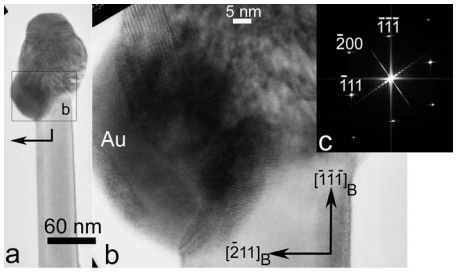

FIG. 5. (a) TEM image of an InAs/GaAs nanowire tip region with its corresponding HRTEM image in (b). (c) A FFT image taken on the GaAs portion in (b).

the lower Au/GaAs $\{111\}_B$ interface energy ($\gamma_{\mathrm{Au/GaAs}\{111\}B}$) than the Au/GaAs $\{111\}_A$ interface energy ($\gamma_{\mathrm{Au/GaAs}\{111\}A}$), i.e., $\gamma_{\mathrm{Au/GaAs}\{111\}B} < \gamma_{\mathrm{Au/GaAs}\{111\}A}$. In fact, this might be the key reason that epitaxial III-V semiconductor nanowires can be readily grown on $\{111\}_B$ substrates. The fundamental reason for lower interfacial energy of the catalyst particles with $\{111\}_B$ surfaces might be related to higher reactivity[17] and higher surface energy of B type surfaces compared to that of A type surfaces.[18,19]

Although the majority of the nanowire morphology is shown in Fig. 3(b), more complicated nanowire morphology can often be observed. An example is shown in Fig. 5(a), in which InAs sections can be identified by the strain contrast and/or the moiré fringes. Since the InAs growth is led by the Au catalysts, the morphology of InAs tracks the movement of the Au catalysts.[10] In Fig. 5(a), InAs segment has grown across the GaAs nanowire sidewalls as indicated by an arrow, whereas in Fig. 3(b) InAs segment has directly grown adjacent and antiparallel to GaAs nanowires.[10] To understand this difference in the motion of the Au catalyst, HRTEM analysis is conducted. Figure 5(b) shows a HRTEM image in the vicinity of the Au catalyst and accompanied InAs and GaAs sections. To understand the crystallographic information, FFT pattern was taken [shown in Fig. 5(c)] on the GaAs section in Fig. 5(b), showing a $\langle 110\rangle$ diffraction pattern. By indexing the diffraction spot parallel to the nanowire growth direction, $(\bar{1}\bar{1}\bar{1})^*$, and its adjacent $(\bar{2}00)^*$ spot, remaining spots can be indexed as described earlier [refer to Fig. 3(f)]. Based on this analysis, we can confirm that the Au catalyst retains a $\{112\}_B$ interface with the sidewall of the GaAs nanowire. These results clearly indicate that though the Au catalysts may originally slide onto $\{112\}_A$ sidewalls, they would ultimately move toward $\{112\}_B$ sidewalls of the GaAs nanowires. This tendency further supports our anticipation that $\gamma_{\mathrm{Au/GaAs}\{111\}B} < \gamma_{\mathrm{Au/GaAs}\{111\}A}$.

It should be mentioned that twins are often observed in nanowires; particularly they lie on the atomic planes perpendicular to the growth direction.[14] However, these twins are rotation twins, i.e., their existence does not alter the growth direction being $[\bar{1}\bar{1}\bar{1}]$, but rather alter the polarity of nanowire sidewalls by $n\times 60°$ rotation (where n is an integer) of the nanowire segments separated by a rotation twin.[14] As a consequence, a twinning causes a $n\times 60°$ rotation in each $\{112\}$ sidewall, which in turn causes each $\{112\}_A$ or $\{112\}_B$, respectively, to become $\{112\}_B$ or $\{112\}_A$ with a rotation twin

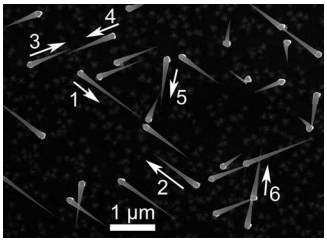

FIG. 6. SEM image showing top view of branched InAs/GaAs nanowire heterostructures. The electron beam is perpendicular to the substrate surface.

in between. This crystallographic possibility features totally six possible $\langle 112\rangle_A$ and six possible $\langle 112\rangle_B$ directions for nanowires grown $\{111\}_B$ surfaces. As a result, InAs branches evolve along six possible $\langle 111\rangle_B$ directions (other than $[\bar{1}\bar{1}\bar{1}]$),[11] all developed from $\{112\}_B$ sidewalls. Figure 6 shows such a case, where the six branch directions are marked by the arrows. If these twins can be eliminated as suggested by Joyce *et al.*,[20] it is possible to limit the directions of branches by half. Based on this analysis, design and growth of branched nanowire heterostructures with desired directions become possible.

It should be emphasized that these observations not only provide important scientific insights to understand the behavior of catalysts during the growth of nanowire heterostructures but also offer technologic guidelines for design and manufacturing of nanowire heterostructure based devices. For example, branched nanowire heterostructures can be realized by depositing catalysts on a nanowire and the subsequent growth.[21,22] If the facets of sidewalls of stem nanowires are polar, there will be distinct sidewalls for the catalysts to preferentially stay on. Such a preference can be used to design regular branched nanowire arrays. Moreover, this preference may also be used to integrate the nanowires systematically, for example, using diffusion bonding of the Au particles.[23]

IV. SUMMARY

In this study, the crystallographic movement behavior of Au catalysts during growth of InAs on GaAs nanowires is carefully investigated using TEM. It has been found that Au catalysts preferentially retain an interface with GaAs on their $\{112\}_B$ sidewalls. This crystallographically driven preference is attributed to the different interface energies between these two polar {112} interfaces. This phenomenon can be used to design the regular branched nanowire arrays.

ACKNOWLEDGMENTS

The Australian Research Council is acknowledged for the financial support of this project. One of the authors (M.P.) acknowledges the support of an International Postgraduate Research Scholarship. The Australian National Fabrication Facility established under the Australian Government's National Collaborative Research Infrastructure Strategy is also acknowledged for access to the facilities for this study.

[1] H. J. Fan, P. Werner, and M. Zacharias, Small **2**, 700 (2006).
[2] A. J. Mieszawska, R. Jalilian, G. U. Sumanasekera, and F. P. Zamborini, Small **3**, 722 (2007).
[3] R. Agarwal and C. M. Lieber, Appl. Phys. A: Mater. Sci. Process. **85**, 209 (2006).
[4] C. J. Novotny, E. T. Yu, and P. K. L. Yu, Nano Lett. **8**, 775 (2008).
[5] H. A. Nilsson, T. Duty, S. Abay, C. Wilson, J. B. Wagner, C. Thelander, P. Delsing, and L. Samuelson, Nano Lett. **8**, 872 (2008).
[6] E. Lind, A. I. Persson, L. Samuelson, and L. E. Wernersson, Nano Lett. **6**, 1842 (2006).
[7] S. A. Dayeh, D. P. R. Aplin, X. T. Zhou, P. K. L. Yu, E. T. Yu, and D. L. Wang, Small **3**, 326 (2007).
[8] R. S. Wagner and W. C. Ellis, Appl. Phys. Lett. **4**, 89 (1964).
[9] N. Wang, Y. Cai, and R. Q. Zhang, Mater. Sci. Eng. R. **60**, 1 (2008).
[10] M. Paladugu, J. Zou, Y. N. Guo, G. J. Auchterlonie, Y. Kim, H. J. Joyce, Q. Gao, H. H. Tan, and C. Jagadish, Small **3**, 1873 (2007).
[11] M. Paladugu, J. Zou, G. J. Auchterlonie, Y. N. Guo, Y. Kim, H. J. Joyce, Q. Gao, H. H. Tan, and C. Jagadish, Appl. Phys. Lett. **91**, 133115 (2007).
[12] M. Paladugu, J. Zou, Y. N. Guo, X. Zhang, Y. Kim, H. J. Joyce, Q. Gao, H. H. Tan, and C. Jagadish, Appl. Phys. Lett. **93**, 101911 (2008).
[13] X. Zhang, J. Zou, M. Paladugu, Y. N. Guo, Y. Kim, H. J. Joyce, Q. Gao, H. H. Tan, and C. Jagadish, Small **5**, 366 (2009).
[14] J. Zou, M. Paladugu, H. Wang, G. J. Auchterlonie, Y. N. Guo, Y. Kim, Q. Gao, H. J. Joyce, H. H. Tan, and C. Jagadish, Small **3**, 389 (2007).
[15] M. T. Bjork, B. J. Ohlsson, T. Sass, A. I. Persson, C. Thelander, M. H. Magnusson, K. Deppert, L. R. Wallenberg, and L. Samuelson, Appl. Phys. Lett. **80**, 1058 (2002).
[16] J. Johansson, B. A. Wacaser, K. A. Dick, and W. Seifert, Nanotechnology **17**, S355 (2006).
[17] H. C. Gatos and M. C. Lavine, J. Electrochem. Soc. **107**, 427 (1960).
[18] D. B. Holt, J. Mater. Sci. **23**, 1131 (1988).
[19] N. Moll, A. Kley, E. Pehlke, and M. Scheffler, Phys. Rev. B **54**, 8844 (1996).
[20] H. J. Joyce, Q. Gao, H. H. Tan, C. Jagadish, Y. Kim, X. Zhang, Y. N. Guo, and J. Zou, Nano Lett. **7**, 921 (2007).
[21] K. A. Dick, K. Deppert, M. W. Larsson, T. Martensson, W. Seifert, L. R. Wallenberg, and L. Samuelson, Nature Mater. **3**, 380 (2004).
[22] Y. Jung, D. K. Ko, and R. Agarwal, Nano Lett. **7**, 264 (2007).
[23] Z. Y. Gu, H. K. Ye, A. Bernfeld, K. J. T. Livi, and D. H. Gracias, Langmuir **23**, 979 (2007).